

# On the collisional depolarization and transfer rates of spectral lines by atomic hydrogen. III: application to $f$ -states of neutral atoms.

M. Derouich<sup>1</sup>, S. Sahal-Br  chot<sup>1</sup>, and P. S. Barklem<sup>2</sup>

<sup>1</sup> Observatoire de Paris-Meudon, LERMA UMR CNRS 8112, 5, Place Jules Janssen, F-92195 Meudon Cedex, France.

<sup>2</sup> Department of Astronomy and Space Physics, Uppsala University, Box 515, S 751 20 Uppsala, Sweden  
e-mail: Moncef.Derouich@obspm.fr

Received 2003 / accepted XXXX

**Abstract.** The theory of collisional depolarization of spectral lines by atomic hydrogen (Derouich et al. 2003a; Derouich et al. 2003b) is extended to  $f$ -atomic levels ( $l=3$ ). Depolarization rates, polarization and population transfer rates are calculated and results are given. Each cross section as a function of the effective quantum number for a relative velocity of  $10 \text{ km s}^{-1}$  is given together with an exponent  $\lambda$ , if it exists, on the assumption that the cross section varies with velocity as  $v^{-\lambda}$ . A general trends of depolarization rates, of polarization transfer rates and of population transfer rates are given. A discussion of our results is achieved.

**Key words.** Sun: atmosphere - atomic processes - line: formation, polarization

## 1. Introduction

The observation of the so-called “second solar spectrum” (a term first suggested by V.V. Ivanov of St. Petersburg, Russia; see Stenflo & Keller 1997; Stenflo et al. 2000; Stenflo 2001; Gandorfer 2000; Gandorfer 2002), which is the spectrum of the linear polarization observed near the limb, is due to the scattering of the underlying anisotropic radiation. The atomic polarization may be modified by several factors, in particular the magnetic field (Hanle effect), and also the isotropic collisions with the neighboring particles of hydrogen. Therefore the depolarization rates, polarization and population transfer rates

by collisions with hydrogen are needed in order to quantitatively interpret the observed polarization in terms of magnetic fields in solar quiet regions.

In Derouich et al. (2003a) and Derouich et al. (2003b) (hereafter Papers I and II, respectively), a semi-classical theory for calculations of depolarization rates, polarization and population transfer rates has been developed and applied to  $p$  ( $l=1$ ) and  $d$  ( $l=2$ ) atomic states. In the present paper we extend this theory to  $f$ -atomic levels ( $l=3$ ). This paper presents the first calculations of the depolarization and the collisional transfer rates for  $f$ -atomic states.

Our semi-classical theory is not specific for a given atom and its application is possible even to heavy atoms (Ti, Fe, ...), for which there are no available depolarization rates and transfer of polarization and population rates data. The extension of this method gives possibility to calculate depolarization and collisional transfer rates of  $p$  ( $l=1$ ),  $d$  ( $l=2$ ) and  $f$  ( $l=3$ ) atomic levels. It should now be possible to rapidly obtain the large amount of data needed for the interpretation of the second solar spectrum. Using our method, general trends of all rates for  $p$  ( $l=1$ ),  $d$  ( $l=2$ ) and  $f$  ( $l=3$ ) atomic levels with orbital angular momentum quantum number  $l$  are able to be discussed for the first time.

## 2. Method

The method used to determine depolarization rates, transfer of polarization and population rates is the same as the one previously introduced in Papers I and II. We denote as  $D^k(nlJ, T)$  the collisional depolarization rate for the statistical tensor of rank  $k$ . Each level of total angular momentum  $J$  relaxes with  $2J+1$  independent depolarization rates. In particular  $D^0(nlJ, T)$  is the destruction rate of population, which is zero since elastic collisions do not alter the population of an atomic level ( $nlJ$ ),  $D^1(nlJ, T)$  is the destruction rate of orientation (circular polarization) and  $D^2(nlJ, T)$  is the destruction rate of alignment (linear polarization) which is of interest in the understanding of the second solar spectrum. If the quenching must be taken into account,  $D^k(nlJ \rightarrow nlJ', T)$  corresponds to collisional transfer of population ( $k=0$ ), orientation ( $k=1$ ) and alignment ( $k=2$ ) (Paper II). Since potentials are computed in the rotating frame, which is obtained from the fixed laboratory frame by means of the geometrical rotation  $R(\beta, \frac{\pi}{2}, \frac{\pi}{2})$ , the interaction potential matrix is diagonal (see, for example, Paper I). The extension of our calculations to  $f$ -atomic levels ( $l=3$ ) requires the determination of seven RSU potentials  $V_{eff,m}$  ( $-3 \leq m \leq 3$ ). For more details we refer to Paper I and Paper II and to the ABO papers (Anstee 1992; Anstee & O'Mara 1991, 1995; Anstee, O'Mara & Ross 1997; Barklem 1998; Barklem & O'Mara 1997; Barklem, O'Mara & Ross 1998). The total wave function  $|\psi\rangle$  of the system is developed over the basis formed by the eigenvectors  $|M_l\rangle$ :

$$|\psi(t)\rangle = \sum_{M_l} a_{M_l}(t) e^{-iE_{M_l}^0 t} |M_l\rangle \quad (1)$$

where  $E_{M_l}^0$  is the energy eigenvalues of the isolated atoms. For  $f$ -states, seven semi-classical coupled linear differential equations describing the evolution of the manifold of states are obtained by writing the time-dependent Schrödinger equation (see Barklem et al. 1998). Having the RSU potentials  $V_{eff,m}$ , after integration of these coupled equations over an entire collision, we obtain the  $a_{M_l}(t)$  coefficients and then the transition  $T$ -matrix elements (Paper I; Paper II). All rates are obtained after integrations, over impact parameters and velocities, of transitions probabilities given by equation (39) in Paper I and equation (11) in Paper II.

### 3. Results

As for  $p$  and  $d$  atomic states calculations, in most cases, the behaviour of the cross sections with the relative velocity  $v$  obeys a power law of the form:

$$\sigma^k(n3J \rightarrow n3J', v)(J = J' \text{ and } J \neq J') = \sigma^k(n3J \rightarrow n3J', v_0) \left(\frac{v}{v_0}\right)^{-\lambda^k(n3J \rightarrow n3J')}, \quad (2)$$

where  $v_0$  is a typical velocity where the cross section is calculated ( $10 \text{ km s}^{-1}$ ). Tables 1 and 2 give respectively variation of cross sections with the effective principal quantum number  $n^*$  and the corresponding velocity exponents. Cross sections for other velocities can be obtained from Tables 1 and 2 using equation (2). Tables 1 and 2 can be interpolated for an appropriate  $n^*$  corresponding to a given observed line in order to obtain the needed rates (Paper I; Paper II). For cross sections obeying equation (2), the collisional depolarization and transfer rates can be expressed by equation (13) of Paper II. Sometimes, especially for the alignment transfer calculations, such behaviour was not obeyed (the cross sections showed oscillations with relative velocities) and so  $\lambda^k(n3J \rightarrow n3J')$  is not reported (Table 2). We have to calculate directly the cross sections for each velocity. The collisional depolarization and transfer rates  $D^k(nlJ \rightarrow nlJ', T)$  ( $J = J'$  and  $J \neq J'$ ) follow from numerical integration over the velocities.

Figure 1 shows the alignment depolarization rates ( $k = 2$ ) as a function of the local temperature  $T$  and  $n^*$  for  $l = 3$ . The population transfer rates ( $k = 0$ ) and the linear polarization transfer rates ( $k = 2$ ) as a function of  $T$  and  $n^*$  are displayed in Figs 2 and 3. All these rates increase with the temperature. For a temperature  $T \leq 10000 \text{ K}$ , the destruction rate of alignment  $D^2(n35/2)/n_H \leq 7 \times 10^{-14} \text{ rad. m}^3 \text{ s}^{-1}$ ,  $D^2(n33)/n_H \leq 12 \times 10^{-14} \text{ rad. m}^3 \text{ s}^{-1}$  and  $D^2(n37/2)/n_H \leq 7 \times 10^{-14} \text{ rad. m}^3 \text{ s}^{-1}$ . The population transfer rate  $D^0(n35/2 \rightarrow n37/2)/n_H \leq 7 \times 10^{-14} \text{ rad. m}^3 \text{ s}^{-1}$  and the linear polarization transfer rate  $D^2(n35/2 \rightarrow n37/2)/n_H \leq 5 \times 10^{-15} \text{ rad. m}^3 \text{ s}^{-1}$ . These numerical values are given for  $n^* \leq 5$  which include most of the lines of interest.

### 4. General trends

For a given effective quantum number  $n^*$ , and for the cases  $l = 1$ ,  $l = 2$ , and  $l = 3$ , destruction rates of alignment are such that  $D^2(n33, T) < D^2(n22, T) < D^2(n11, T)$ .

$n^*$	$\sigma^2(n3\frac{5}{2})$	$\sigma^2(n33)$	$\sigma^2(n3\frac{7}{2})$	$\sigma^0(n3\frac{5}{2} \rightarrow n3\frac{7}{2})$	$\sigma^2(n3\frac{5}{2} \rightarrow n3\frac{7}{2})$
3.3	426	782	491	478	40
3.4	451	831	521	518	44
3.5	489	892	561	565	51
3.6	535	962	603	616	58
3.7	584	1055	654	684	67
3.8	637	1151	708	768	81
3.9	695	1249	765	865	96
4	759	1365	824	962	101
4.1	835	1467	875	1031	110
4.2	890	1572	899	1119	108
4.3	1024	1777	1051	1188	114
4.4	1077	1908	1097	1297	121
4.5	1236	2166	1247	1418	121
4.6	1249	2279	1306	1508	116
4.7	1420	2411	1432	1503	125
4.8	1485	2515	1485	1529	118
4.9	1521	2587	1504	1630	132
5	1928	3135	1845	1786	130

**Table 1.** Variation of the cross sections, for the relative velocity of  $10 \text{ km s}^{-1}$ , with the effective principal number. Cross sections are in atomic units.

A similar result has been obtained for the broadening of spectral lines. In fact, Barklem et al. (1998) have previously shown that, also for a given  $n^*$ , lines with upper  $p$ -states ( $l = 1$ ) are more broadened than lines with upper  $d$ -states ( $l = 2$ ), and similarly lines with upper  $d$ -states are more broadened than lines with upper  $f$ -states ( $l = 3$ ). This effect is similar to that first seen observationally in the solar spectrum by Carter (1949). In general, when the orbital angular momentum quantum number  $l$  increases the depolarization rates and transfer of polarization and population rates decrease for a given value of the energy of the state of the valence electron  $E_{nl}$ .  $E_{nl}$  is related to  $n^*$  by  $n^* = [2(E_\infty - E_{nl})]^{-1/2}$ ,  $E_\infty$  being the binding energy of the ground state.

For  $f$ -states, when  $J = 7/2$  and  $J' = 5/2$  we have:  $D^0(n37/2 \rightarrow n35/2, T) > D^1(n37/2 \rightarrow n35/2, T) > D^2(n37/2 \rightarrow n35/2, T) > D^4(n37/2 \rightarrow n35/2, T) > D^3(n37/2 \rightarrow n35/2, T) > D^5(n37/2 \rightarrow n35/2, T)$ . We recall that  $D^k(n l J \rightarrow n l J', T)$  is a linear combination of  $\zeta(n l J M_J \rightarrow n l J' M_J', T)$  (equation (3) in Paper II). The population transfer rate is the greater transfer rate because for  $k = 0$  the coefficients of this linear combination are positive. These coefficients are constant and equal to  $1/\sqrt{(2J+1)(2J'+1)}$  which leads to a  $D^0(n l J \rightarrow n l J', T)$  which is proportional to  $\zeta(n l J \rightarrow n l J', T)$  (equation (5) in Paper II). However, the sign of the coefficients of the

$n^*$	$\lambda^2(n3\frac{5}{2})$	$\lambda^2(n33)$	$\lambda^2(n3\frac{7}{2})$	$\lambda^0(n3\frac{5}{2} \rightarrow n3\frac{7}{2})$	$\lambda^2(n3\frac{5}{2} \rightarrow n3\frac{7}{2})$
3.3	0.228	0.277	0.301	0.280	-
3.4	0.249	0.295	0.315	0.283	-
3.5	0.252	0.303	0.325	0.288	-
3.6	0.260	0.311	0.331	0.289	-
3.7	0.275	0.329	0.346	0.289	-
3.8	0.275	0.334	0.354	0.296	-
3.9	0.282	0.342	0.367	0.301	0.103
4	0.306	0.363	0.402	0.320	0.117
4.1	0.298	0.362	0.412	0.344	0.176
4.2	0.278	0.336	0.384	0.351	0.267
4.3	0.240	0.306	0.333	0.370	0.328
4.4	0.235	0.304	0.319	0.394	0.384
4.5	0.262	0.333	0.349	0.415	0.396
4.6	0.215	0.317	0.311	0.440	0.411
4.7	0.181	0.289	0.284	0.435	0.497
4.8	0.192	0.268	0.269	0.409	0.600
4.9	0.218	0.248	0.268	0.363	0.587
5	0.222	0.224	0.242	0.331	0.500

**Table 2.** Velocity exponents  $\lambda^k(nlJ \rightarrow nlJ')(J = J' \text{ and } J \neq J')$  corresponding to the cross sections of Table 1.

linear combination for transfer rates of rank  $k \geq 1$  is sometimes positive and sometimes negative. For example, these coefficients have the sign of  $M_J \times M'_J$  for orientation transfer rates ( $k = 1$ ) and the sign of  $(3M_J^2 - J(J+1)) \times (3M_J'^2 - J'(J'+1))$  for alignment transfer rates. The other coefficients of the linear combination for  $k > 2$  may be obtained on request from the authors. We conclude that, for  $k \neq 0$ , the collisional transfer rates may be positive or negative as a function of transition probabilities between the Zeeman sublevels which depend on  $n^*$ . The depolarization rates are usually positive.

All rates were found to increase with temperature  $T$ . The functional form  $D(T) = AT^{(1-\lambda)/2}$  may be accurately fitted to the depolarization rates and the population transfer rates (Paper I; Paper II). However, sometimes the collisional transfer rates with  $k \neq 0$ , cannot be fitted by the power-law  $AT^{(1-\lambda)/2}$  and so  $\lambda$  is not reported (Table 2 in the present paper and Table 2 in Paper II). This is due to the fact that these collisional transfer rates are the sum of incoherent contributions from the states  $|nlJM_J\rangle$  and  $|nlJ'M_J'\rangle$ . We notice that the above remarks are valid also for  $p$  and  $d$ -atomic states.

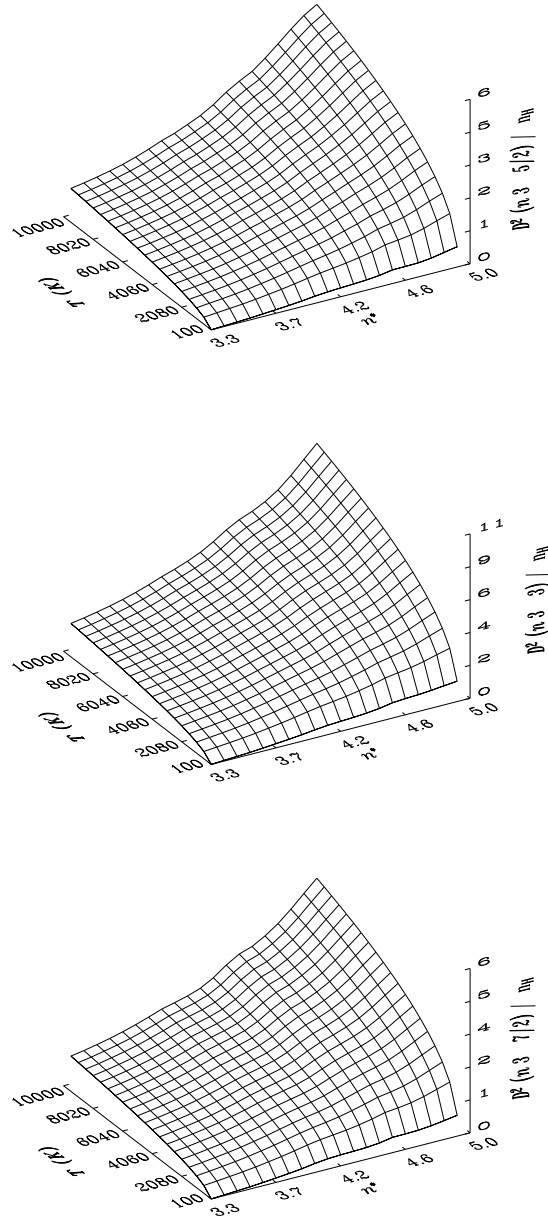


**Fig. 1.** Depolarization rates per unit H-atom density as a function of temperature  $T$  and  $n^*$ . For  $l = 3$ , each figure:  $S = \frac{1}{2}$  and  $J = \frac{5}{2}$ ;  $S = 0$  and  $J = 3$ ;  $S = \frac{1}{2}$  and  $J = \frac{7}{2}$ . Depolarization rates are given in  $10^{-14}$  rad.  $\text{m}^3 \text{s}^{-1}$ .

## 5. Discussion

Unfortunately, there is neither experimental nor quantum chemistry depolarization and collisional transfer rates for  $f$ -states for comparison. We expect that the main differences between the RSU potentials and those from quantum chemistry, which are considered as more realistic, occur at the short-range interactions. We have verified that these close collisions do not influence the computed depolarization and collisional transfer rates for

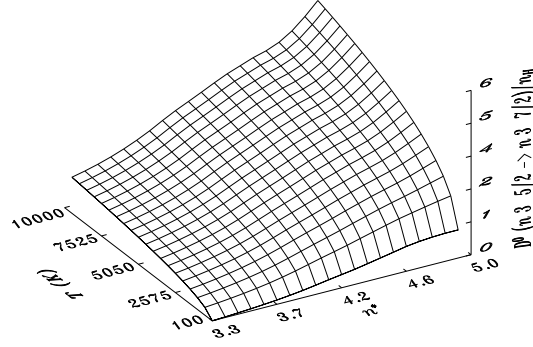


**Fig. 2.** Population transfer rate per unit H-atom density ( $k=0$ ) as a function of temperature  $T$  and  $n^*$ .  $l = 3$ ,  $S = \frac{1}{2}$ ,  $J = \frac{5}{2}$  and  $J' = \frac{7}{2}$ . Population transfer rate is given in  $10^{-14}$  rad.  $\text{m}^3 \text{s}^{-1}$ .

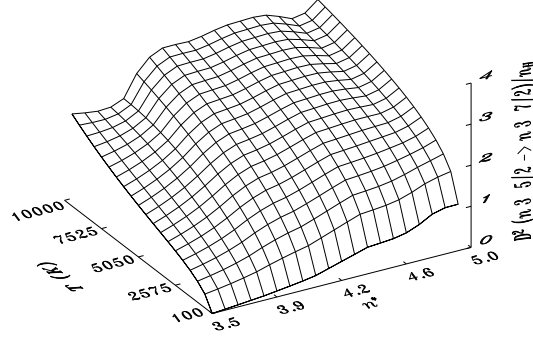


**Fig. 3.** Linear polarization transfer rate per unit H-atom density ( $k=2$ ) as a function of temperature  $T$  and  $n^*$ .  $l = 3$ ,  $S = \frac{1}{2}$ ,  $J = \frac{5}{2}$  and  $J' = \frac{7}{2}$ . Linear polarization transfer rate is given in  $10^{-15}$  rad.  $\text{m}^3 \text{s}^{-1}$ .

$f$ -states. The decisive contribution to the depolarization and collisional transfer rates calculations occurs at intermediate-range interactions. In Paper I, which is concerned with  $p$ -states, comparison with quantum chemistry results in Kerkeni (2002) gives depolarization rates in agreement to better than 20 %. Extrapolating our results obtained for  $p$  and  $d$  states (Paper I; Paper II), we expect a rather good agreement (relative difference less than 20 % at solar temperatures) between our rates obtained for  $f$ -states and a full quantum mechanical treatment.

## 6. Conclusion

This paper is a continuation of a series concerned with the theoretical calculations of the depolarization and collisional transfer rates. Thanks to the extension to  $f$ -atomic states

( $l = 3$ ), we are able to obtain the first general conclusions concerning trends of all rates as a function of orbital angular momentum quantum number  $l$ . An extrapolation for  $l > 3$  would be useful for a more complete interpretation of the “second solar spectrum”. This work is in progress. An extension of our theory to the case of ions will be the subject of further papers.

## References

- Anstee S.D., & O’Mara B.J., 1991, MNRAS, 253, 549
- Anstee S.D. PhD thesis, Univ. Queensland, 1992
- Anstee S.D., & O’Mara B.J., 1995, MNRAS, 276, 859
- Anstee S.D., O’Mara B.J., & Ross J.E., 1997, MNRAS, 284, 202
- Barklem P.S., & O’Mara B.J., 1997, MNRAS, 290, 102
- Barklem P.S., & O’Mara B.J., & Ross J.E., 1998, MNRAS, 296, 1057
- Barklem P.S. PhD thesis , Univ. Queensland, 1998
- Carter W.W., 1949, Phy. Rev., 76, 962
- Derouich M., Sahal-Br  chot S., Barklem P.S., & O’Mara B.J., 2003a, A&A, 404, 763 (Paper I)
- Derouich M., Sahal-Br  chot S., Barklem P.S., 2003b, in press, A&A (Paper II)
- Gandorfer A., 2000, The Second Solar Spectrum: A high spectral resolution polarimetric survey of scattering polarization at the solar limb in graphical representation, vol. 1: 4625 Å to 6995 Å (Hochschulverlag AG an der ETH Zurich)
- Gandorfer A., 2002, The Second Solar Spectrum: A high spectral resolution polarimetric survey of scattering polarization at the solar limb in graphical representation, vol. 2: 3910 Å to 4630 Å (Hochschulverlag AG an der ETH Zurich)
- Kerkeni B., 2002, A&A, 390, 791
- Stenflo J.O., & Keller C.U., 1997, A&A, 321, 927
- Stenflo J.O., Keller C.U., & Gandorfer A., 2000, A&A, 355, 789
- Stenflo J.O., 2001, in Advanced Solar Polarimetry: Theory, Observation, and Instrumentation, ed. M. Sigwarth (San Francisco: Astronomical Society of the Pacific), ASP Conf. Ser., 236, 97